

## Experimental Analysis on Aluminium Alloys (7xxx) After Friction Stir Processing for Engineering Applications

P. K. Mandal, John Felix Kumar, Merrin J Varkey

Department of Metallurgical and Materials Engineering, Amal Jyothi College of Engineering, Kanjirappally-686518, Kerala, India.

### ABSTRACT

The high strength Al-Zn-Mg alloys (7xxx series) have some specific properties such as spontaneous ageing nature, high strength-to-weight ratio and effect of Sc addition makes it hard. This alloy is largely used in aircraft and automobile industries. Scandium (Sc) addition in aluminium alloys have great technological advantages to reducing the cast grain sizes and generate large volume fraction of constituent particles ( $Al_3Sc$ ) and promoting the precipitation of a more uniform dispersoid distribution. The grain refinement effect and the age-hardening behaviour of Al-Zn-Mg alloys are studied on the basis of Optical microscopy (OM), Field emission scanning electron microscopy (FESEM), Transmission electron microscopy (TEM) and Vicker's hardness measurements. Friction stir processing (FSP) is an emerging surface-engineering solid state technology which locally eliminates casting defects and refines microstructure to enhance specific properties to some considerable depth. During FSP, the severe plastic deformation and thermal exposure of material significantly enhanced microstructural changes. FSP results in significant temperature rise within and around the processed zone. The stir zone (SZ) grains suggest effective strains together with a microstructural evolution that occurs by a combination of plastic deformation and a dynamic recovery or recrystallization. The temperature rise of 450-500°C has been noted within the SZ for aluminium alloys. Intense plastic deformation and temperature rise results in significant microstructural evolution, therefore, fine recrystallized grains of  $10.97 \pm 1.45 \mu m$ , precipitate dissolution and coarsening, textural changes and micro residual stresses. In general, processed zone is characterized by a recrystallized fine grain with uniformly distributed  $\eta$  and  $Al_3Sc$  particles. So, FSP enhances mechanical properties many folds as comparison to heat treated aluminium alloys. In this regard, many researchers have proposed energy-based model for the FSW/FSP in their experimental work. Finally, the mechanical properties have been evaluated after FSP and estimated likely to 0.2% proof strength increase to 200.2%, ultimate strength increase to 231.1%, ductility increase to 125.5%, and hardness increase to 17.7% as compared to  $T_4$  condition, respectively.

**KEY WORDS:** Scandium addition, grain refinement, FSP,  $T_4$  heat treatment, energy-based model, mechanical properties.

Date of Submission: 30-09-2020

Date of Acceptance: 13-10-2020

### I. INTRODUCTION

The aluminium alloys (7xxx series) are used for many engineering applications due to natural age-hardening ability, good corrosion resistance, and good fracture resistance [1, 2]. The weight reduction is the primary criteria for light weight alloys because approximately of 100 kg. weight reduction means saving of up to 0.5 liters of fuel per every 100 km. Similar advantages may be achieved as a replacement for parts made of steels reducing the unit weight of structure by 10 to 50% for aluminium alloys. The weight reduction is critical for aerospace industry because the tensile strength after appropriate ageing treatment reaches more than 600 MPa with good fracture resistance. The precipitation sequences of aluminium alloys (7xxx series) as reported in the literature are as follows:  $\alpha(SSSS) \rightarrow$  coherent stable GP zone  $\rightarrow$  semicoherent intermediate  $\eta(Mg_2Zn_{11}) \rightarrow$  incoherent stable  $\eta(MgZn_2)$  or  $T(AlMg_4Zn_{11})$ . An important characteristic feature of the Al-Zn-Mg alloy is exhibiting low quench sensitivity. The quenching rate after solution treatment only has a small effect on the mechanical properties and properties mostly obtained after ageing treatment. Also, quenching sensitivity depends on (Zn+Mg) content and Zn/Mg ratio [3-5]. Main strengthening mechanisms are likely to solid solution, age-hardening (coherency strain hardening, chemical hardening, and dispersion hardening), and grain refinement by inoculation effects. The chemical composition can contain the following phases are  $\alpha$ -solid solution,  $\beta$ -phase ( $Al_8Mg_5$ ),  $\tau$ -phase ( $Al_2Zn_3Mg_3$ ),  $\eta$ -phase ( $MgZn_2$ ).  $\beta$  phase is formed for magnesium-rich alloys, while occurring of  $\tau$ ,  $\eta$  phases depends on proportion between zinc and magnesium contents. The dispersion hardenings of Al-Zn-Mg alloys are a complicated process and it is assumed that the dispersion particles of  $\eta$  phase and GP zone are responsible for their high strength properties at low temperature.

The aluminium alloys containing zinc exhibit high solubility indicates no lattice distortion for formability point of view and also achieve high strength after accelerating artificial ageing than the natural ageing. The accelerated ageing provides less susceptibility to stress corrosion than the natural ageing, and it is possible for increasing ageing temperature. Most hardening achieved for 140-150°C for 6h ageing time for Al-Zn-Mg alloy. The significant loss of strength occurs at elevated temperatures for 160-200°C, and this is the most detrimental feature of aluminium alloys [6-8]. But strain hardening occurs for those alloys do not response to age hardening for example of 1xxx, 3xxx, 5xxx series are usually strengthening by strain hardening which have generally involved by cold working. It can be observed that the maximum of precipitate volume fraction occurs for this type of alloy as temperature range from 140-150°C. Such large amount of precipitate will play important role in the precipitation hardening. The strengthening that results from such ageing occurs because the solute retained in the supersaturated solid solution forms precipitates, as part of an equilibrium response, which are finely dispersed throughout the grains and increase the ability of the material to resist deformation by the process of slip. Maximum hardening or strengthening occurs when the ageing treatment leads to the formation of critical dispersions of one or more of these fine precipitates. The grain refinement of aluminium alloys is achieved by the addition of inoculants particles (e.g. Al<sub>3</sub>Sc) in the form of Al-2wt% Sc master alloy [9-12]. Inoculation is particularly wide practised in the aluminium industry. Sc has been attributed to the strong grain refining influence of the Al<sub>3</sub>Sc phase, which leads to nucleation of a large number of grains at a low undercooling. When the activation energy for precipitation and the number of nucleation sites are both considered, heterogeneous nucleation is favoured at lower undercoolings and the homogeneous nucleation is favoured at higher undercoolings [13, 14].

In addition, fine grain promotes the flow of molten metal to feed shrinkage during solidification, resulting in smaller and more uniform dispersed shrinkage or gas porosities. Fine grains also provide a complex network of grain boundaries, reducing tendency for hot crack initiation and propagation. The patented concept of Friction stir welding (FSW) in the 1990's opened a new field for joining metals, especially light alloys and FSP emerged around this concept. Processed surfaces have enhanced mechanical properties, such as hardness, tensile strength, fatigue, corrosion and wear resistance. A uniform equiaxed fine grain structure is obtained improving superplastic behaviour. Also, there are several theoretical energy-based models have been exercised such as Khandkar et al. [2003, 2006], Heurtier et al. [2006], Hamilton et al. [2008] for FSW/FSP and conclusions are drawn for heat energy as per experimental parameters [15-18]. The aim of this work is to examine in detail the potential useful effects of adding Sc from 0.21 to 0.63 wt.% to aluminium alloys (7xxx series), influencing for grain refinement and dispersoid optimization as well as to examine FSP is mostly used to locally eliminate casting defects and refine microstructures in selected locations, for property improvements and component performance enhancement. The purpose of this paper is to provide theoretical and experimental basis for many engineering applications of these new aluminium alloys.

## II. MATERIALS AND EXPERIMENTAL STUDY

**Table 1:** Chemical composition (7xxx series) analysed by ICP-MS (Inductively coupled plasma mass spectroscopy) and AAS (Atomic absorption spectroscopy) methods of studied alloys (in wt. %).

Alloy nos.	Zn	Mg	Sc	Si	Fe	Al	Zn+Mg	Zn/Mg	IADS/AAA Designation
Alloy 1	6.19	1.86	0.21	0.05	0.08	Bal.	8.10	3.33	7000
Alloy 2	5.30	3.00	0.25	0.11	0.10	Bal.	8.30	1.77	7000
Alloy 3	5.65	1.98	0.63	0.03	0.26	Bal.	7.63	2.85	7075

\*IADS = International Alloy Designation System, and AAA- Aluminium Alloy Association.

The results of the present investigation have been discussed under the following alloys development such as preparation of Al-Zn-Mg alloys using scandium inoculation, and grain refinement effects of aluminium alloys due to Sc inoculants, and reason for hardness and mechanical properties variation of alloys during different heat treatments. The aluminium alloys have been developed as per flow chart as shown in Figure 1. The charge usually consists of commercially pure aluminium cut into small pieces and put into a graphite crucible in an electrical muffle furnace at 780°C for 3h melting time. Pieces of scandium were added in a graphite crucible as a form of master alloy (Al-2wt.%Sc), which added carefully before pouring of liquid metal into a mild steel mould (size: 200×90×24 mm<sup>3</sup>) and controlled fading of scandium as well as vaporization of Mg and Zn during adding in liquid metal. As Sc was added in the alloys as different compositions of 0.45 wt.%, 0.7 wt.%, and 0.9 wt.%, respectively. But recovery of Sc obtained around 50 to 60 wt.% after wet chemical analysis as shown in Table 1. The ageing kinetics for present alloys were studied at 120 to 180°C to achieve optimum hardness in a reasonable period of time. The as-cast alloys were selected for solution treatment at 465°C for 1h then immediately followed by water quenching (T<sub>4</sub>) and subsequently aged at 120, 140, 160, and 180°C for 16h (T<sub>6</sub>) to each alloy, respectively. The as-cast and heat-treated alloys were subjected to metallographic studies. The optical microstructures (OM) were revealed to as-cast, T<sub>4</sub>, and after double-pass FSP alloys as per standard metallographic procedures and etched with the Keller's reagent (1% HF+1.5% HCl+2.5% HNO<sub>3</sub>+95% distilled

water) for following the light microscopy as shown in Figure 3, Figure 5, and Figure 6. The TEM samples were prepared initially thinning down around less than 100  $\mu\text{m}$  by gently mechanically polishing then preferred for electrolytically etching (solution of 75%  $\text{CH}_3\text{OH}$  + 25%  $\text{HNO}_3$ , 12V, and  $-35^\circ\text{C}$ ) to make them thinner for final TEM observations as shown in Figure 4. The FESEM microstructures were examined through light microscopy and followed for EDS analysis for confirmation of scandium segregation on grain boundary areas as shown in Figure 5. The Vicker's hardness measurement (10 kg. load) to evaluate the strength or hardening effect as solution treated condition as well as  $T_6$  alloys. The solution treated ( $T_4$ ) samples were selected for artificial ageing at different temperatures such as 120, 140, 160, and  $180^\circ\text{C}$  for 16h to each alloy, respectively. Each time average six hardness values randomly were taken instance on aged samples and following sequences of ageing time maintain thoroughly as 1h, 2h, 4h, 6h, 8h, 10h, 12h, and 16h, respectively. Finally, hardness data was tabulated and calculated activation energies ( $E_a$ ) based on ageing temperatures from 120 to  $180^\circ\text{C}$  and specified time from the Arrhenius equation. The solution treated ( $T_4$ ) plate was fixed firmly on the vertically standing milling machine with predetermined parameters such as 1000 rpm of tool rotation speed (clockwise and unidirectional), 70 mm/min traverse speed, double-pass, with specified tool design such as pin diameter 3 mm, pin height 3.5 mm with oval shape of tip, pin shoulder diameter 20 mm, total tool length 75 mm and it made of hardened martensitic stainless steel ( $211\text{HV}_{30\text{kg}}$ ). A cross sectional view AA of pin plunged into the working plate has been shown alongside of FSP set-up in Figure 2(a). The entire double-pass FSP process has been schematically shown in Figure 2(a-c) and steps are followed thoroughly during processing. The FSP is an integral process which main working plate not be deformed, no noise, no fume generation and it can be considered as a solid state green technology. Experimental samples were collected from processed zone and machined for tensile samples preparation as per ASTM: E8/E8 M-11 standard. The tensile testing was carried out in an Universal Testing Machine (UTM) (25 kN, H25 K-S, UK) with cross head speed of 1 mm/min at room temperature and results are exhibited in the bar diagrams as shown in Figure 6(c).

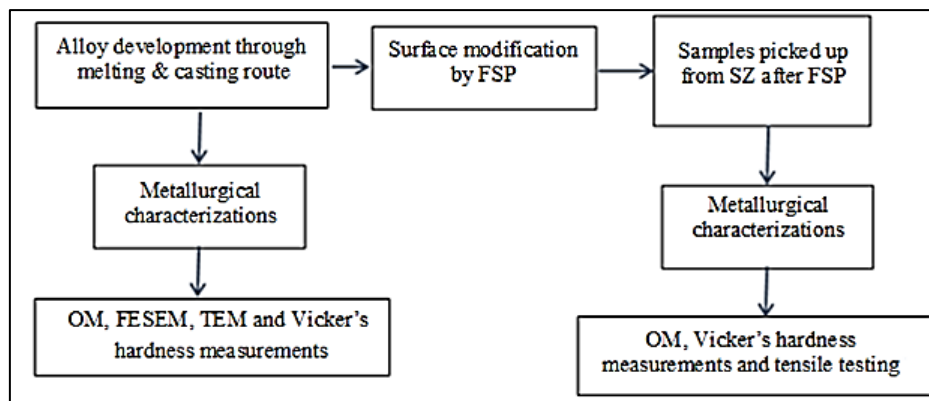


Fig. 1: A complete flow chart for Al alloys preparation and their double-pass FSP.

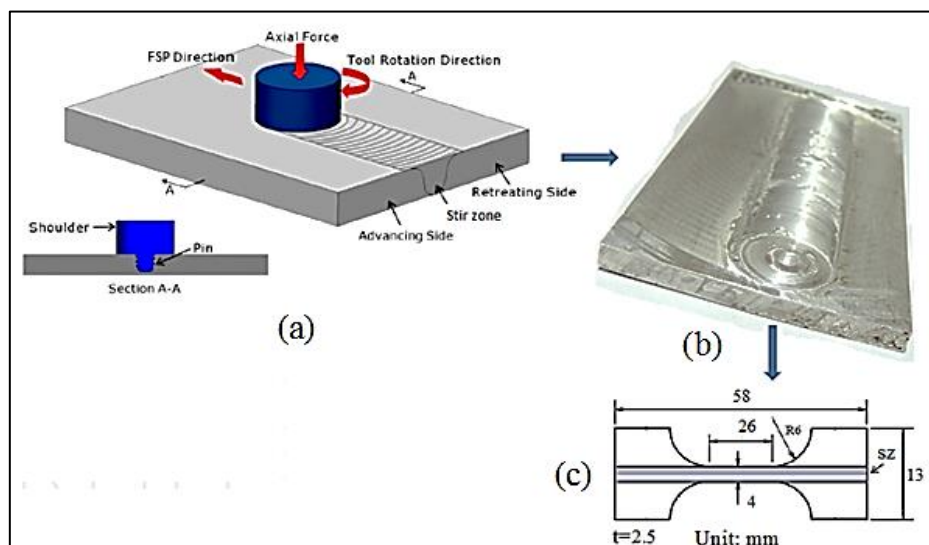


Fig. 2: Schematic diagrams of (a) FSP set-up, (b) Double-pass FSP (35% deviation from the first pass to second pass during processing) plate (size:  $150 \times 90 \times 8 \text{ mm}^3$ ), (c) Tensile test-piece as per ASTM std.: E8/E8 M-11.

### **III. RESULTS AND DISCUSSION**

#### **Inoculation effects of scandium in aluminium alloys**

The microstructures and properties of Al-Zn-Mg alloys are strongly affected by adding small quantities of scandium. Significantly grain refinements in castings are obtained by promoting heterogeneous nucleation during solidification, such that the transition from columnar to equiaxed grain growth is favoured. This is achieved by providing many efficient heterogeneous nucleation sites in the melt, which constitutes the basis for grain refinement. Scandium forms a high melting eutectic phase with aluminium at 655°C (0.55wt%Sc), Al<sub>3</sub>Sc (L<sub>2</sub> type) having FCC crystal structure and a lattice parameter close to that of aluminium. Scandium additions greater than 0.55wt.% (i.e., hypereutectic, L→ $\alpha$ -Al+Al<sub>3</sub>Sc) have been shown the result in fine grain enhancement in aluminium alloys, suggesting that the primary Al<sub>3</sub>Sc phase serves as an effective grain nucleant [19-22]. The presence of impurity contents (Fe, Si) also affect the primary Al<sub>3</sub>Sc particles number, size, size distribution, and density in the melt of aluminium alloys. Silicon impurity increases the Al<sub>3</sub>Sc precipitation kinetics and density in aluminium. These particles are extremely fine, homogeneously distributed (~10-20 nm) and approximate density similar to GP zones. Therefore, controlling impurities and their concentrations can enhance the grain refinement of aluminium alloys.

#### **Main strengthening mechanisms of aluminium alloys**

The mechanism of strengthening alloys through age hardening involves impeding the motion of dislocation. Dislocations are apparently stabilized most effectively when the cluster of solute atoms is coherent with the crystal structure of the solvent, i.e., the solute atoms are collected into a cluster but still have the same crystal structure as the solvent phase. This causes a great deal of strain because of mismatch in size between the solvent and solute atoms. The cluster stabilized dislocations, because dislocations tend to reduce the strains, similar to the reduction is strain energy of a single solute atom by a dislocation. When the dislocations are anchored by coherent solute clusters, the alloys are considerably strengthened and hardened. There are several advantages of using Sc in aluminium alloys. The effect of Sc additions will of course depend on the composition of the alloys. Strengthening mechanisms can be achieved such as grain refinement during casting, increase strength from Al<sub>3</sub>Sc particles, resistance to recrystallization, and superplastic properties. The aged structure and the kinetics of ageing depends on both the Zn and Mg concentration and the temperatures of solution and ageing treatments and so on. As the Sc content increases within the specified solubility in the solid solution, the grains virtually do not disintegrate. The maximum solubility of Sc increases from 0.20 to 0.63 wt.% at present in studied aluminium alloys. When the amount of Sc exceeds the eutectic content, there may be agglomeration tendency for Al<sub>3</sub>Sc particles but still the grains disintegrate to the finest possible size [23-26].

#### **Microstructural refinement through FSP and ageing treatments**

In addition, the FSP is used for localized modification and microstructural control of surface layers of processed metallic components for specific property enhancement. Processed surfaces have shown an improvement of mechanical properties, such as hardness and tensile strength, better fatigue, corrosion and wear resistance. This technique has been successfully applied in the production of fine grained structure and surface composite [Ma et al., 2008; Nascimento et al., 2009; Kwon et al., 2003; Colligan et al., 1999] [27, 28]. Figure 3(a-c) shows optical microstructures of cast aluminium alloys achieved fine grains in addition of minor Sc contents for Alloy 1 is 72.0  $\mu$ m of 0.21%Sc, for Alloy 2 is 28.10  $\mu$ m of 0.25%Sc, and for Alloy 3 is 13.73  $\mu$ m of 0.63%Sc, respectively. Grain refinement has been achieved for gradually refine the grains due to minor Sc addition to hypereutectic content of Sc (>0.55%), because there is maximum possibility of heterogeneous nucleation sites generated when the amount of Sc exceeds the eutectic content, still may be agglomeration tendency for Al<sub>3</sub>Sc particles existence in FESEM analysis for Alloy 3 in Figure 5(c). Indicated numerous Sc content is 27.41wt.%. Figure 3(d-f) shows optical microstructures of T<sub>6</sub> aluminium alloys exhibited laterally coarse grains with fine precipitates and eliminated grain boundary segregation due to two steps heat treatments such as solution treatment and later on low temperature ageing treatments (>200°C), when existence of grain achievement for Alloy 1 is 27.82  $\mu$ m, for Alloy 2 is 24.04  $\mu$ m, and Alloy 3 is 14.03  $\mu$ m, respectively. But Alloy 3 exhibited finest grain size due to hypereutectic content of Sc (>0.55%) addition as well as ample amount of Al<sub>3</sub>Sc particles generation with grain boundary pinning effects at this ageing condition as shown in Figure 3(f).

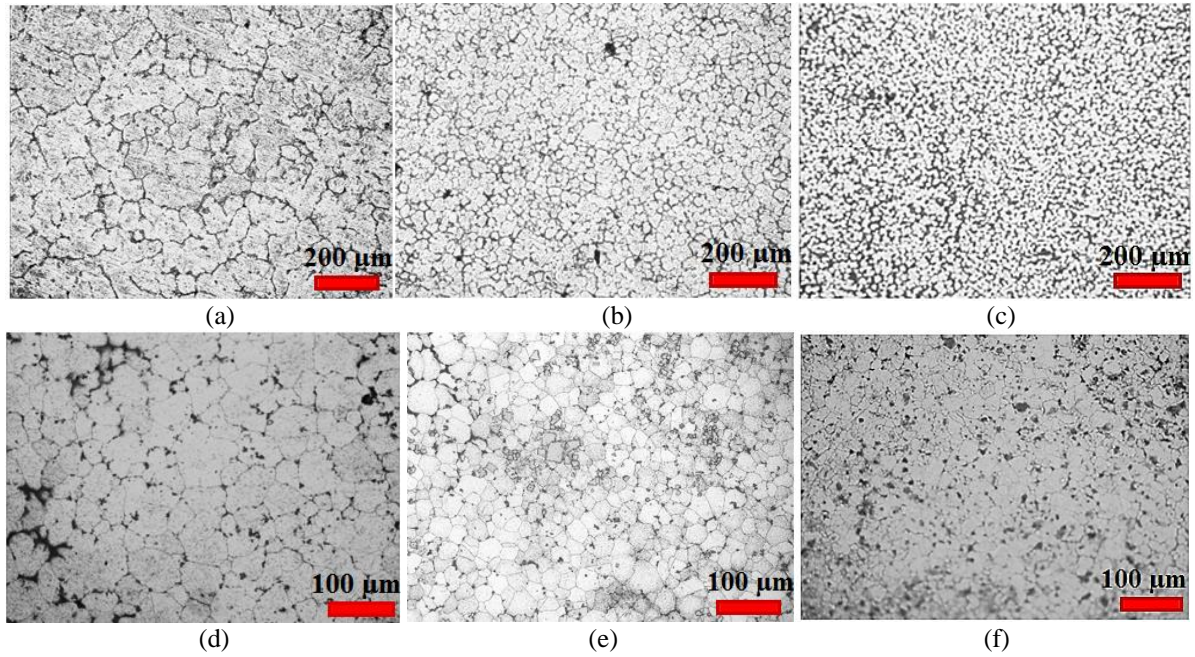


**Fig. 3:** Optical microstructures of as-cast Al alloys: (a) Alloy 1, (b) Alloy 2, (c) Alloy 3; Optical microstructures of T<sub>6</sub> Al alloys: (d) Alloy 1 (aged at 160°C for 2h), (e) Alloy 2 (aged at 140°C for 6h), (f) Alloy 3 (aged at 160°C for 2h).

#### TEM and FESEM analysis

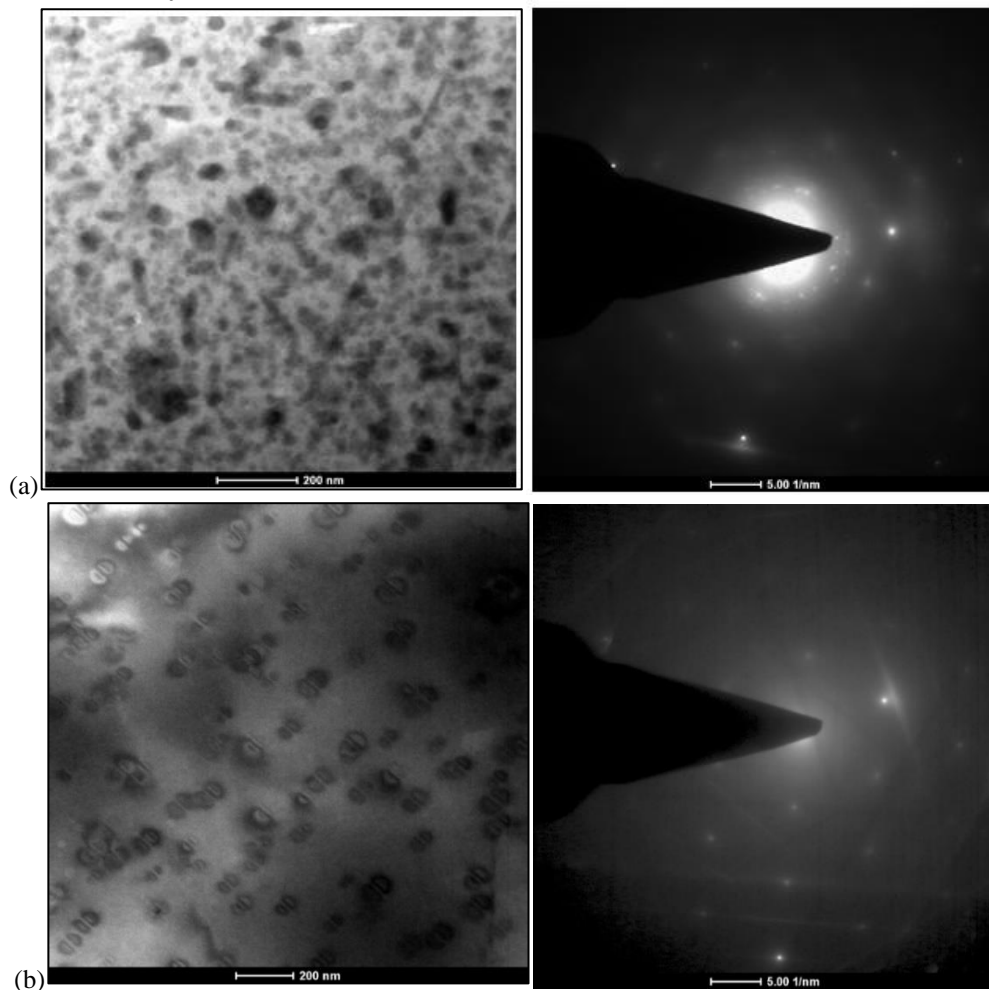


**Fig. 4:** TEM microstructures with SAD analysis of T<sub>6</sub> (aged at 140°C for 6h) Al alloys: (a) Alloy 2, (b) Alloy 3.

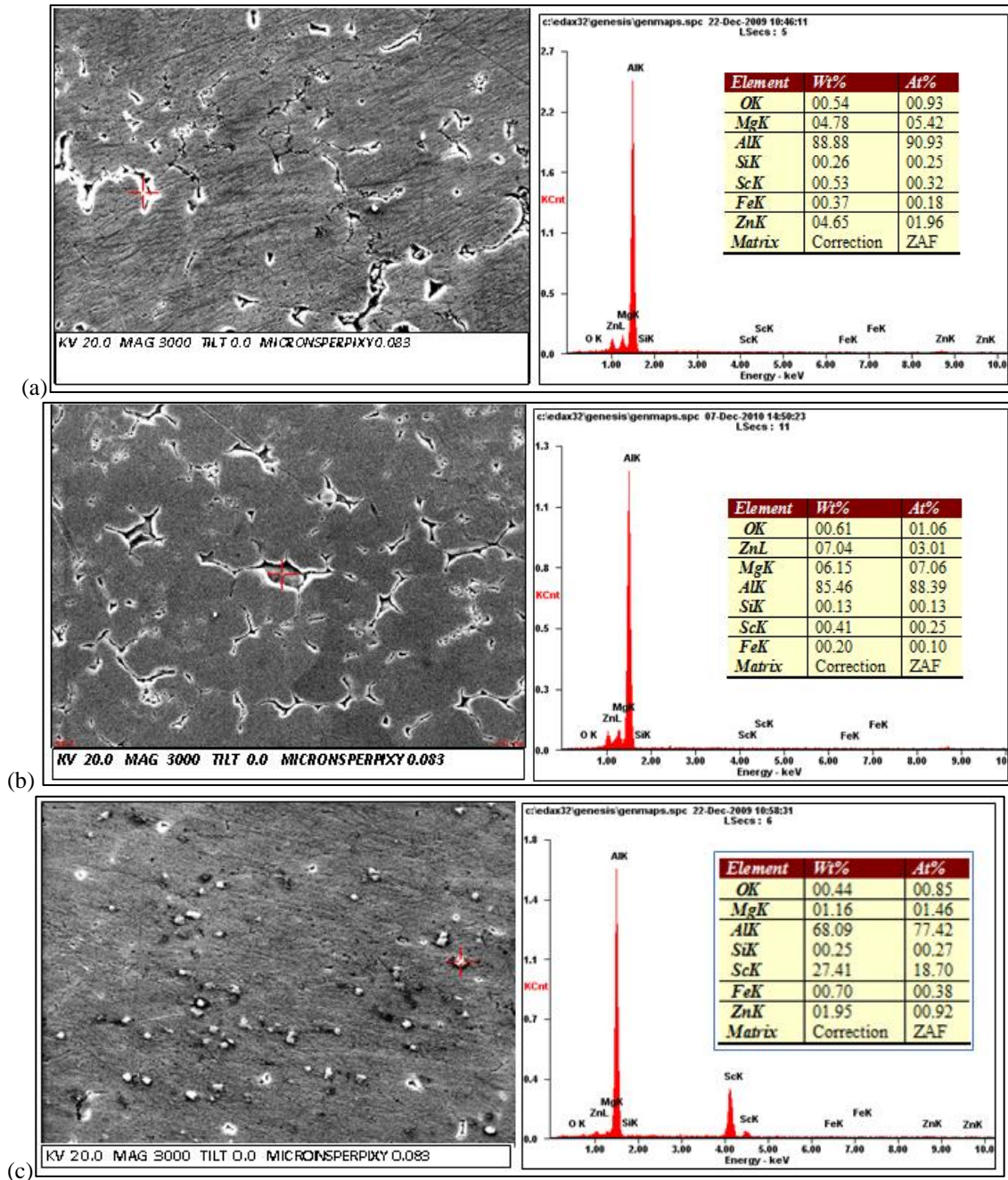


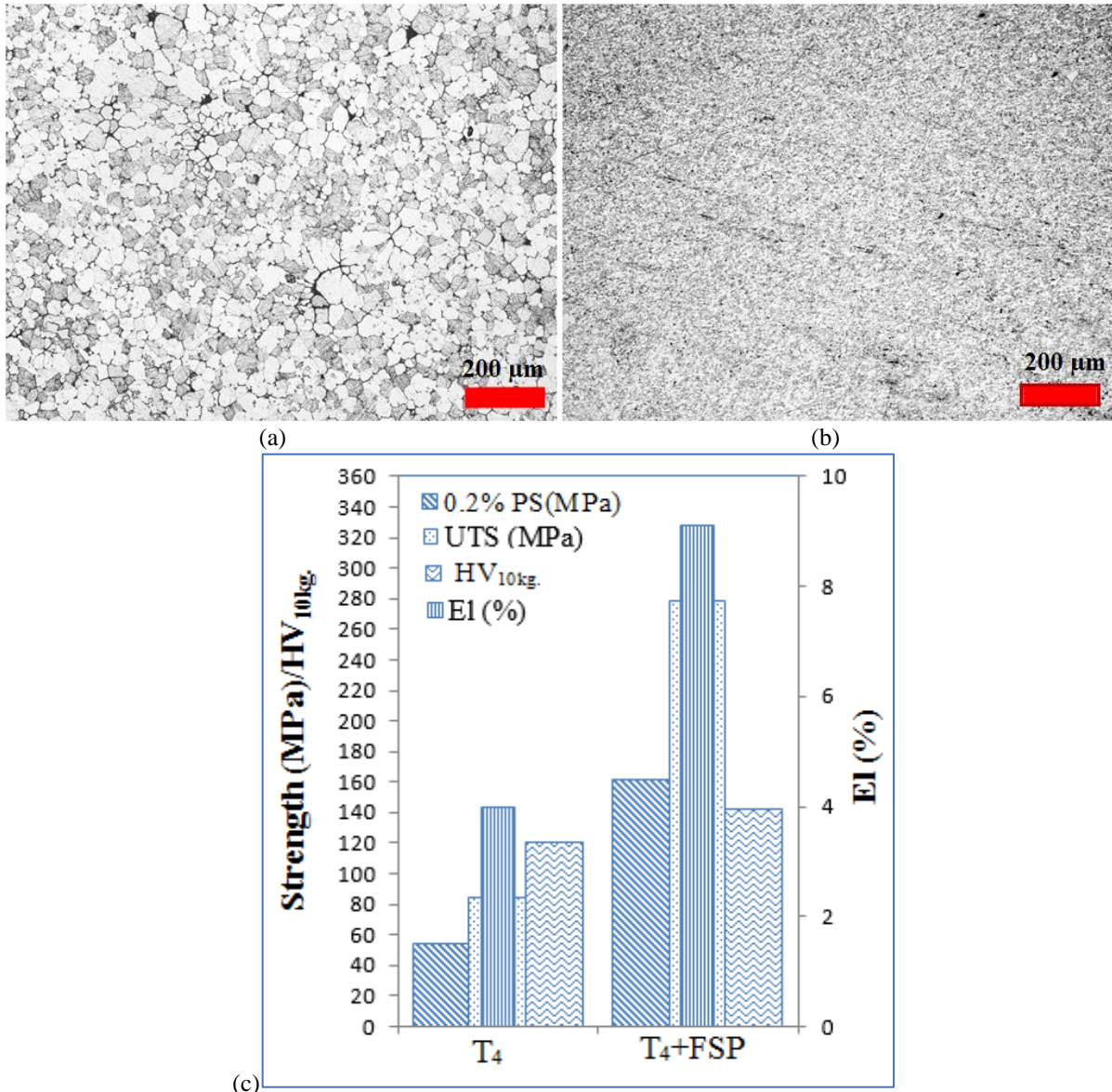
Fig. 5: FESEM with EDS analysis of as-cast Al alloys: (a) Alloy 1, (b) Alloy 2, (c) Alloy 3.

Figure 4(a) shows TEM micrograph with SAD analysis of  $T_6$  aluminium Alloy 2 exhibited fine distribution of precipitates with  $Al_3Sc$  particles and T phases agglomeration tendency in matrix. There are several black spots for as-cast porosities and inhomogeneities with large coarse particles agglomeration dominate in matrix for Alloy 2. Figure 4(b) shows TEM microstructure with SAD analysis of  $T_6$  aluminium Alloy 3 exhibited uniform distribution, identical shape and size of cauliflower type  $Al_3Sc$  particles in matrix. Figure 5(a-c) shows FESEM with EDS analysis of as-cast aluminium alloys exhibited typical grain boundary segregation of impurity elements as well as agglomeration tendency of high Sc content of 27.42 wt.% (hypereutectic content) of Alloy 3 as shown in Figure 5(c).

#### Energy-based models analysis and mechanical properties of FSP aluminium alloys

The activation energy of precipitation had also been measured by the changes of hardness with ageing time and temperatures (120 to 180°C) using the Arrhenius relationship, i.e.,  $\Delta HV = \Delta HV_0 \exp(-E_a/RT)$  [29, 30]. Therefore, the activation energy values are found to be quite low from experimental results as around 7.42 kJ/mole at 10h ageing time. Low activation energies indicated that driving force of the precipitation process is

slow and minor Sc addition enhances the precipitation process in aluminium alloys. Figure 6(a) shows optical microstructure of solution treated ( $T_4$ ) aluminium Alloy 2 with grain size achieved of  $36.34 \pm 8.1 \mu\text{m}$ , it seems grain growth occur after  $T_4$  heat treatment because the numerous soluble phases formed during solidification can be re-dissolved into the matrix. The precipitation strengthening is attributed to the dissolving of the coarse second phase particles during the solution treatment which may offer large amounts of solution atoms and is beneficial for the precipitation in the subsequent ageing treatment. Figure 6(b) shows optical microstructure of  $T_4$ +FSP aluminium Alloy 2 with grain size achieved of  $10.97 \pm 1.45 \mu\text{m}$  in SZ region. It is noted that during FSP three distinct process regions have been identified such as stir zone (SZ) is centre zone of tool pin size (3 mm), and thermo-mechanically affected zone (TMAZ) is adjacent to SZ region, where the metal is plastically deformed as well as heated to a temperature for insufficient of recrystallization. Then, the heat affected zone (HAZ) is exposed by the frictional heat generated between the tool and workpiece and no mechanical deformation occurred [31-33]. The fine-grain is achieved due to dynamic recrystallization mechanism for  $\text{Al}_3\text{Sc}$  precipitate particles with  $\eta$  or  $\text{T}(\text{Al}_2\text{Zn}_3\text{Mg}_3)$  type hardening phases play vital roles during high temperature deformation, and also the high density dislocations which stored at immediate vicinity of these particles have the source of dynamic recrystallization [34, 35]. There are several theoretical energy-based models have been studied such as Khandkar et al. [2003, 2006], Heurtier et al. [2006], Hamilton et al. [2008] for FSW/FSP of aluminium alloys. The total energy generated per unit length of the FSP is the sum of the energy generated due to friction between the tool and the workpiece and the plastic deformation within the workpiece. An empirical formula developed a proposed energy model by Hamilton et al.,  $\frac{T_{max}}{T_s} = 1.56 \times 10^{-4} E_{eff} + 0.54$ ; where  $T_{max}$  is the maximum temperature generated within the FSP,  $T_s$  is the solidus temperature in Kelvin,  $E_{eff}$  is the effective energy generated per unit length of FSP in J/mm. As per many literatures supported and Hamilton energy model can be concluded  $T_s = 636^\circ\text{C}$  [from Al-Zn equilibrium phase diagram] and  $T_{max} = 500^\circ\text{C}$  [from present experimental parameters 1000 rpm, 70 mm/min], it can be put into above equation to obtain  $E_{eff} = \frac{T_{max}}{T_s} \left( \frac{10^4}{1.56} \right) - 0.54$  (J/mm); and it can be easily calculated to  $E_{eff} = 5448.18$  J/mm. As per Hamilton et al. [2009] proposed model during FSW/FSP temperature is equal to the solidus temperature of aluminium alloy, i.e.,  $\frac{T_{max}}{T_s} = 1$ . So, from the above equation it can be calculated easily to  $E_{eff} = 6409.72$  J/mm. As per Khandkar's torque-based model that is good agreement with heat energy generated is a function of applied force, coefficient of friction between the tool and the workpiece, tool dimensions, and FSW/FSP parameters [36]. In case of FSW/FSP process parameters the heat input is given by the relation as follows [37]: heat input,  $q = \frac{2\pi}{3s} \times \mu \times p \times \omega \times R_s \times \eta$ ; where  $q$  is the heat generated in J/mm;  $\mu$  is co-efficient of friction = 0.3;  $p$  = normal force of 15 kN;  $\omega$  = rotational speed in 16.67 rev/s;  $R_s$  = shoulder radius in m;  $s$  = traverse speed in mm/s;  $\eta$  = heat transfer efficiency = 0.8;  $s = 70 \text{ mm/min} = 1.17 \text{ mm/s}$ ;  $R_s$  = shoulder diameter of 0.02 m; and it can be calculated from the above equation to  $q = 2150$  J/mm. The experimental heat input may be high value of 2150 J/mm as comparison to several theoretical energy-based models. Also, in an optical microstructure (Figure 6.b) clearly indicated numerous black spots after FSP may be due to Zn vaporization effect. Thus, a comparison between the estimated heat energy and its corresponding maximum temperature obtained using the different energy-based proposed models and the experimental result shows a good agreement. Figure 6(c) shows the bar diagrams have exhibited the results of mechanical properties of aluminium Alloy 2 at  $T_4$  and  $T_4$ +FSP conditions. The  $T_4$  aluminium Alloy 2 exhibited around 0.2% proof strength of 58 MPa, ultimate tensile strength of 82 MPa, Vicker's hardness of 121 HV, and elongation of 3.8%, respectively. The solution heat treatment implies homogeneous distribution of soluble second phase particles, and eliminates grain boundary segregation and re-dissolve coarse precipitates into the matrix. The precipitation strengthening is the main strengthening mechanism along with low lattice mismatch with inoculated particles, and coherent dispersoids of  $\text{Al}_3\text{Sc}$  particles. Consequently, comparative study shows that  $T_4$ +FSP aluminium Alloy 2 exhibited the mechanical properties increasing likely to 0.2% proof strength increase to 200.2%, ultimate strength increase to 231.1%, ductility increase to 125.5%, and hardness increase to 17.7%, respectively. The overall mechanical properties are increased due to refined grains ( $10.97 \pm 1.45 \mu\text{m}$ ), porosity elimination and fine precipitates ( $\text{Al}_{12}\text{Mg}_7$ ) and  $\text{Al}_3\text{Sc}$  dispersoids. But hardness marginally decreases due to high elongation and dense SZ after FSP [38-41].



**Fig. 6:** Illustration of optical microstructures of Al alloy: (a) T<sub>4</sub> condition, and (b) SZ of T<sub>4</sub>+FSP condition for Alloy 2; (c) The bar diagram exhibited mechanical properties of Al alloy: T<sub>4</sub>; T<sub>4</sub> +FSP conditions for Alloy 2.

#### IV. CONCLUSION

Significant grain refinement has been achieved in high strength Al-Zn-Mg alloys (7xxx series) with minor addition of scandium from 0.21 to 0.63 wt.% through melting route. The Al<sub>3</sub>Sc particles with the structure of L1<sub>2</sub> precipitating from the matrix during solution treatment, pin dislocation restricts the nucleation of recrystallization which leads to strengthening of these alloys. The tensile properties of Al-Zn-Mg-Sc alloys appreciably have been improved after solution treatment and subsequently ageing treatment by precipitation hardening or age hardening process. The TEM micrographs with SAD analysis of T<sub>6</sub> aluminium alloy has exhibited fine distribution of precipitates with Al<sub>3</sub>Sc particles and T phases agglomeration tendency even though for low Sc content (0.25%) aluminium alloy. The optical microstructure exhibited optimum finer grain size (10.97±1.45 μm) in SZ region after T<sub>4</sub>+FSP aluminium alloy. The fine-grain is achieved due to dynamic recrystallization mechanism for Al<sub>3</sub>Sc precipitate particles with η or T(Al<sub>2</sub>Zn<sub>3</sub>Mg<sub>3</sub>) type hardening phases during high temperature deformation (450-500°C), and also the high density dislocations which stored at immediate vicinity of these particles have the source of dynamic recrystallization. There are several theoretical energy-based models have been studied such as Khandkar et al. [2003, 2006], Heurtier et al. [2006], Hamilton et al. [2008] for FSW/FSP of aluminium alloys. As per Hamilton energy model, it can be concluded  $T_s = 636^\circ\text{C}$  [from Al-Zn equilibrium phase diagram] and  $T_{max} = 500^\circ\text{C}$  [from present experimental parameters 1000 rpm, 70 mm/min], and it can be easily calculated to  $E_{eff} = 5448.18 \text{ J/mm}$ . Consequently, in case of FSW/FSP process parameters the heat input is calculated as 2150 J/mm for experimental aluminium alloys. The experimental heat

input may be high value (2150 J/mm) as compared to several theoretical energy-based models. The overall mechanical properties have been increased due to refined grains ( $10.97 \pm 1.45 \mu\text{m}$ ), porosity elimination and fine precipitates (T,  $\text{Al}_{12}\text{Mg}_7$ ) and  $\text{Al}_3\text{Sc}$  dispersoids.

### ACKNOWLEDGEMENTS

This research paper has presented for new technological views with the financial support of the Ministry of Human Resource Development (MHRD) fellowship provided by the Department of Metallurgical and Materials Engineering at Indian Institute of Technology Roorkee (IITR), Uttarakhand-247667, India.

### REFERENCES

- [1]. T. Engdahl, V. Hansen, P.J. Warren, K. Stiller, "Investigation of fine scale precipitates in Al-Zn-Mg alloys after various heat treatments" *Materials Science and Engineering A* 327 (2002), pp. 59-44.
- [2]. P. Priya, D.R. Johnson, M.J.M. Krane, "Modeling phase transformation kinetics during homogenization of aluminium alloy 7050", *Computational Materials Science* 138 (2017), pp. 277-287.
- [3]. T. Ungar, J. Lendvai, I. Kovacs, "The decomposition of the solid solution state in the temperature range 20 to 200°C in an Al-Zn-Mg alloy", *Journal of Materials Science* 14 (1979), pp. 671-679.
- [4]. M. Nishi, K. Matsuda, N. Miura, K. Watanabe, S. Ikeno, T. Yoshida, S. Murakami, "EFFECT OF THE Zn/Mg RATIO ON MICROSTRUCTURE AND MECHANICAL PROPERTIES IN Al-Zn-Mg ALLOYS", *Materials Science Forum*, Vols. 794-796 (2014), pp. 479-482.
- [5]. N.M. Han, X.M. Zhang, S.D. Liu, D.G. He, R. Zhang, "Effect of solution treatment on the strength and fracture toughness of aluminium alloy 7050", *Journal of Alloys and Compounds* 509 (2011), pp. 4138-4145.
- [6]. G. Sha, A. Cerezo, "Early-stage precipitation in Al-Zn-Mg-Cu alloy (7050)", *Acta Materialia* 52 (2004), pp. 4503-4516.
- [7]. H. Löffler, I. Kovacs, J. Lendvai, "Review Decomposition processes in Al-Zn-Mg alloys", *Journal of Materials Science* 18(1983), pp. 2215-2249.
- [8]. T. Hu, K. Ma, T.D. Toppling, J.M. Schoenung, E.J. Lavernia, "Precipitation phenomena in an ultrafine-grained Al alloy", *Acta Materialia* 61 (2013), pp. 2163-2178.
- [9]. S. Costa, H. Puga, J. Barbosa, A.M.P. Pinto, "The effect of Sc additions on the microstructure and age hardening behaviour of as cast Al-Sc alloys", *Materials and Design* 42(2012), pp. 347-352.
- [10]. F.A. Costello, J.D. Robson, P.B. Prangnell, "The Effect of Small Scandium Additions to AA7050 on the As-cast and Homogenized Microstructure", *Materials Science Forum*, Vols. 396-402 (2002), pp. 757-762.
- [11]. Y.W. Riddle, T.H. Sanders, Jr., "A study of Coarsening, Recrystallization, and Morphology of Microstructure in Al-Sc-(Zr)-(Mg) Alloys", *Metallurgical and Materials Transactions A*, Vol. 35A, (January 2004), pp. 341-350.
- [12]. P.K. Mandal, R. Anant, R. Kumar, V.M.R. Muthaiah, "Effect of scandium on ageing kinetics in cast Al-Zn-Mg alloys", *Materials Science and Engineering A* 696 (2017), pp. 257-266.
- [13]. Y.W. Riddle, T.H. Sanders, Jr., "Contribution of  $\text{Al}_3\text{Sc}$  to Recrystallization in Wrought Al-Sc Alloys", *Materials Science Forum*, Vols. 331-337 (2000) pp. 939-944.
- [14]. A.L. Greer, A.M. Bunn, A. Tronche, P.V. Evans, D.J. Bristow, "MODELLING OF INOCULATION OF METALLIC MELTS: APPLICATION TO GRAIN REFINEMENT OF ALUMINIUM BY Al-Ti-B", *Acta Materialia*, 48 (2000) 2823-2835.
- [15]. M.S. Wegłowski, S. Dymek, C.B. Hamilton, "Experimental investigation and modelling of Friction Stir Processing of cast aluminium alloy AlSi9Mg", *Bulletin of the Polish Academy of Sciences Technical Sciences*, Vol. 61, No.4, (2013), pp. 893-904.
- [16]. M. Imam, V. Racherla, K. Biswas, "Effect of post-weld natural aging on mechanical and microstructural properties of friction stir welded 6063-T4 aluminium alloy", *Materials and Design* 64 (2014), pp. 675-686.
- [17]. C. Hamilton, A. Sommers, S. Dymek, "A thermal model of friction stir welding applied to Sc-modified Al-Zn-Mg-Cu alloy extrusions", *International Journal of Machine Tools & Manufacture* 49 (2009), pp. 230-238.
- [18]. F. Nascimento, T. Santos, P. Vilaca, R.M. Miranda, L. Quintino, "Microstructural modification and ductility enhancement of surfaces modified by FSP in aluminium alloys", *Materials Science and Engineering A* 506 (2009), pp. 16-22.
- [19]. L-M. Wu, W-H. Wang, Y-F. Hsu, S. Trong, "Effects of homogenization treatment on recrystallization behaviour and dispersoid distribution in an Al-Zn-Mg-Sc-Zr alloy", *Journal of Alloys and Compounds* 456 (2008), pp. 163-169.
- [20]. Z. Heng-hua, "Crystallography and refining mechanism of (Ti, B)-contained salts in pure aluminium", *Transactions of Nonferrous Metals Society of China*, 18(2008), pp. 836-841.
- [21]. P.K. Mandal, "Heat Treatment and Friction Stir Processing Effects on Mechanical Properties and Microstructural Evolution of Sc Inoculated Al-Zn-Mg Alloys", *Materials Science and Metallurgy Engineering*, Vol. 4, No.1, (2017), pp. 16-28.
- [22]. J.H. Li, B. Oberdorfer, S. Wurster, P. Schumacher, "Impurity effects on the nucleation and growth of primary  $\text{Al}_3(\text{Sc}, \text{Zr})$  phase in Al alloys", *Journal Materials Science*, 49 (2014), pp. 5961-5977.
- [23]. X-y. Dai, C-q. Xia, A-r. Wu, X-m. Peng, "Influence of Scandium on Microstructures and Mechanical Properties of Al-Zn-Mg-Cu-Zr Alloys", *Materials Science Forum*, Vols. 546-549 (2007), pp. 961-964.
- [24]. Y. Deng, Z. Yin, K. Zhao, J. Duan, Z. He, "Effects of Sc and Zr microalloying additions on the microstructure and mechanical properties of new Al-Zn-Mg alloys", *Journal of Alloys and Compounds* 530 (2012), pp. 71-80.
- [25]. H. Zhenbo, Y. Zhimin, L. Sen, D. Ying, S. Baochuan, Z. Xiang, "Preparation, microstructure and properties of Al-Zn-Mg-Sc alloy tubes", *Journal of Rare Earths*, Vol. 28, No. 4, (August 2010), pp. 641-645.
- [26]. M.R. Clinch, S.J. Harris, W. Hepples, N.J.H. Holroyd, M.J. Lawday, B. Noble, "Influence of Zinc to Magnesium Ratio and Total Solute Content on the Strength and Toughness of 7xxx series Alloys", *Materials Science Forum*, Vols. 519-521, (2006), pp. 339-344.
- [27]. A. Kurt, I. Uygur, E. Cete, "Surface modification of aluminium by friction stir processing", *Journal of Materials Processing Technology* 211 (2011), pp. 313-317.
- [28]. Z. Zhang, H.W. Zhang, "Numerical studies on the effect of transverse speed in friction stir welding", *Materials and Design* 30 (2009), pp. 900-907.
- [29]. A. Juhasz, I. Kovacs, J. Lendvai, P. Tasnadi, "Initial clustering after quenching in AlZnMg alloys", *Journal of Materials Science* 20(1985), pp. 624-629.
- [30]. W. Sha, "Activation energy for precipitation hardening and softening in aluminium alloys calculated using hardness and resistivity data", *Physica Status Solidi(a)* 203, No. 8, (2006), pp. 1927-1933.

- [31]. C.G. Rhodes, M.W. Mahoney, W.H. Bingel, M. Calabrese, "Fine-grain evolution in friction-stir processed 7050 aluminium", *Scripta Materialia* 48(2003), pp. 1451-1455.
- [32]. M-H. Ku, F-Y.Hung, T-S.Lui, L-H. Chen, W-T. Chiang, "Microstructural Effects of Zn/Mg Ratio and Post Heat treatment on Tensile Properties of Friction Stir Process (FSP) Al-xZn-yMg Alloys", *Materials Transactions*, Vol. 53, No. 5, (2012), pp. 995-1001.
- [33]. M.S. Weglowski, "An experimental study on the Friction Stir Processing process of aluminium alloy", *Key Engineering Materials*, Vols. 554-557 (2013), pp. 1787-1792.
- [34]. J-Q. Su, T.W. Nelson, C.J. Sterling, "Microstructure evolution during FSW/FSP of high strength aluminium alloys", *Materials Science and Engineering A* 405 (2005), pp. 277-286.
- [35]. X. Feng, H. Liu, S.S. Babu, "Effect of grain size refinement and precipitation reactions on strengthening in friction stir processed Al-Cu alloys", *Scripta Materialia* 65 (2011), pp. 1057-1060.
- [36]. J.B. Patel, "Simulation of Peak Temperature & Flow Stress during FSW of Aluminium Alloy AA6061 for Various Tool Pin Profiles", *International Journal of Materials Science and Engineering*, Vol. 2, No. 1, (June 2014), pp. 67-71.
- [37]. A. Kumar, S.S. Gautam, A. Kumar, "HEAT INPUT & JOINT EFFICIENCY OF THREE WELDING PROCESSES TIG, MIG AND FSW AA6061", *International Journal of Mechanical Engineering and Robotics Research*, Vol. 1, No. 1, (January 2014), pp. 89-94.
- [38]. P. Cavaliere, A. Squillace, "High temperature deformation of friction stir processed 7075 aluminium alloy", *Materials Characterization*, 55, 2005, pp. 136-142.
- [39]. K. Ihara, Y. Miura, "Dynamic recrystallization in Al-Mg-Sc alloys", *Materials Science and Engineering A*, 387-389, pp. 647-650.
- [40]. P.K. Mandal, "Investigation of Microstructure And Mechanical Properties of Al-Zn-Mg and Al-Zn-Mg-Sc Alloys After Double Passes Friction Stir Processing", *International Journal of Materials Science and Engineering*, Vol. 5, No.2, June 2017, pp. 47-59.
- [41]. F.C. Liu, Z.Y. Ma, F.C. Zhang, "High Strain Rate Superplasticity in a Micro-grained Al-Mg-Sc Alloy with Predominant High Angle Grain Boundaries", *Journal of Materials Science and technology*, 28(11), 2012, pp. 1025-1030.

P. K. Mandal, et. al. "Experimental Analysis on Aluminium Alloys (7xxx) After Friction Stir Processing for Engineering Applications." *The International Journal of Engineering and Science (IJES)*, 9(9), (2020): pp. 26-35.